Journal of the Ceramic Society of Japan 116 [10] 1115-1120 2008 Paper

Crystallization behavior of optical fibers with multi layered structure for nonlinear optical devices

Naoki IWAFUCHI,* Hirokazu MASAI,* Yoshihiro TAKAHASHI,* Takumi FUJIWARA,*,† Seiki OHARA,*, Yuki KONDO** and Naoki SUGIMOTO****

*Department of Applied Physics, Tohoku University, 6-6-05, Aoba, Sendai 980-8579
**Research Center, Asahi glass Co., Ltd., 1150, hazawa-chou, kanagawa-ku, Yokohama 221-8755

We examined the crystallization behavior of double clad fiber composed by BaO–TiO_2–GeO_2–SiO_2 based glasses in detail. Formation of needle-like fresnoite-type $Ba_2Ti(Ge,Si)_2O_8$ were observed at the interface between the first and second clad. In addition, we employed the two-step heat-treatment (i.e., 728°C, 20 h + 749°C, 1 h) in fabrication of the crystallized fiber in order to obtain the highly-oriented fresnoite phase in the fiber structure. The first treating temperature, 728°C, which gives the maximum nucleation rate, was determined by differential thermal analysis. It was demonstrated that the two-step heat-treatment was effective for improvement of the orientation of fresnoite-type phase in the first clad of the double clad fiber.

Key-words : Optical device, Glass ceramics, Nonlinear optics

[Received June 11, 2008; Accepted September 11, 2008]

1. Introduction

Since the crystallized glass (glass-ceramics) consists of both disordered and ordered region, i.e., glass and crystal phase, it is expected that such material possesses a unique physical property that originate from the crystal phase. Particularly, the crystallized glasses exhibiting second-order optical nonlinearity are one of the most attractive materials for future optical devices because these have a great potential for the active glass-based fiber device. Recently, several research groups succeeded in fabricating the transparent crystallized glasses with the second-order optical nonlinearity.[1)-3)] For example, transparent fresnoite-type $Ba_2TiGe_2O_8$ surface-crystallized glasses fabricated from $30BaO \cdot 15TiO_2 \cdot 55GeO_2$ (BTG55) glass showed the largest second-order nonlinear optical constant, d value, comparable to that of the $LiNbO_3$ single crystal.[4)] In these crystallized glasses, self-organized c-orientation of the fresnoite-type phase is formed at the surface of BTG55 glass, and this is expected to be an origin of the large optical nonlinearity. Orientation structure at the surface of crystallized glass is often explained by a geometric selection effect.[5),6)] According to the geometric selection, crystallite with a preferential growth direction, which is perpendicular to the surface, are finally survives through the crystallization process. The orientation of the crystallized phase at the glass surface is a characteristic of the glass, which indicates a strong tendency of the surface-crystallization (i.e., inhomogeneous nucleation). Very recently, using the self-organized orientation, the crystallized glass fiber with a peculiar structure was fabricated by Hane et al. from the BTG55 glass.[7)] In this crystallized fiber, the fresnoite-type $Ba_2TiGe_2O_8$ (BTG) crystallites with c-axis orientation grew from the surface to the interior. Since the BTG-crystallized glass fiber showed strong second-harmonic generation (SHG), it is expected to be a candidate for a novel optical material.

† Corresponding author: T. Fujiwara; E-mail: fujiwara@laser.apph.tohoku.ac.jp

We have suggested the fiber-type variable optical attenuator (VOA) device as an application of the crystallized glass fiber to a novel fiber-type optical device. For the purpose of equalizing the intensities of propagated optical signals in different network paths before amplification of erbium-doped optical fiber, the VOA is one of the most fundamental optical devices in recent optical telecommunication. The VOA fiber we proposed has three-layer structure consisting of the glass core for wave guide, the first clad with crystalline phase aiming to change in refractive index by the electro-optic effect (EO effect), and the over coated second clad for increase in mechanical strength (see **Fig. 1**). The glass compositions of core, first and second clad region correspond to the molar ratio $30BaO \cdot 10TiO_2 \cdot 2.5Nb_2O_5 \cdot 30GeO_2 \cdot 22SiO_2 \cdot 3La_2O_3 \cdot 1.55Bi_2O_3 \cdot 0.2CeO_2$, $30BaO \cdot 15TiO_2 \cdot 30GeO_2 \cdot 25SiO_2 \cdot 1.0CuO$, and $30BaO \cdot 15TiO_2 \cdot 30GeO_2 \cdot 25SiO_2$, respectively.[8)] Particularly, the first clad composition was decided to crystallize only the first clad region by heat treatment and to achieve the optical attenuation by refractive index change from the EO effect. The refractive indices (at 1.55 μm) of core, first and second clad are 1.788, 1.784 (crystallized region), and 1.746 respectively, and single-mode propagation was confirmed on the fabricated glass fiber with core diameter of 6.5 μm.[9)]

In the EO-type device, low electric power consumption is one of the notable characteristics. Since the electric power consumption of the EO effect is zero in principle, the VOA device using EO effect is expected to reduce both of electric power consumption and running costs compared to a conventional thermo-optic (TO) device. Comparing to conventional single-crystal-based devices, one of the merits of proposed fiber-type VOA is good connectivity to the glass optical fiber circuit, and it leads to provide the easy device assembly.

In the case of device assembly in single crystal, accurate alignment of the crystal direction with the electric field is necessary to utilize a desired EO coefficient effectively. However, since the proposed VOA device has the radially oriented crystal structure, it is not necessary to settle the fiber in the certain direction.

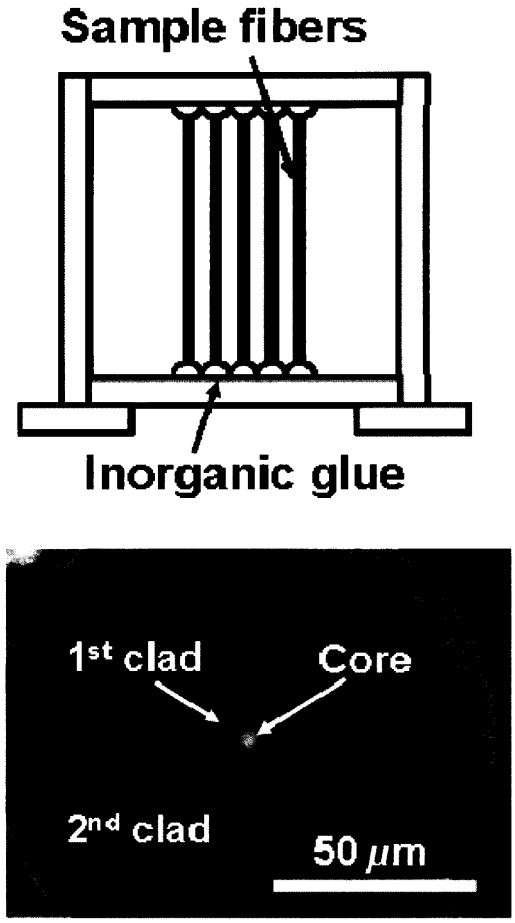

Fig. 1. Illustration for fiber holder and micrograph for the double clad glass fiber.

Therefore, the structure of proposed VOA eliminates effort of the alignment for the device assembly. Furthermore, this device structure allows us to use the anisotropy of electro-optic coefficient. Under the homogeneous electric field, TE and TM mode propagation light will be affected by different refractive indexes. The different refractive indexes cause the phase difference between the two modes, and it will change the polarization state of propagation light. This suggests that the polarization state can be controlled by the external electric field, and it will read to novel optical devices.

One of the most important points in the multi-structural fiber-type VOA is the high orientation to polarization axis of crystallites on the first clad region. Since crystallization behavior and morphology affects the second order optical nonlinearity, research for crystallization behavior and determination of heat treatment conditions are required. Therefore, in this study, the crystallization behavior of the multi-structural glass fibers was investigated to achieve the high orientation of polarization axis in several heating conditions.

2. Experimental procedure

The multi-structural glass fiber was drawn from the preform glass rods fabricated from the glasses with compositions above mentioned.[9] Figure 1 shows the cross section of the double clad glass fiber fabricated in this study. The diameter of core, inner first clad, and outer second clad region were estimated to be ~6.5, 24.5, and 125 μm, respectively. For research of crystallization behavior, heat treatment of the glass fibers was attempted on several heat-treatment conditions using an electric furnace. The sample holder made from alumina was used to fix the fiber samples as shown in Fig. 1. The temperature of crystallization onset, T_x, of the first clad glass were estimated by a differential thermal analysis (DTA) operated at a heating rate of 10 K/min. The glass fibers were heat-treated at the temperatures ranging from $T_x - 50$ K to T_x for 1 h. Morphology of crystallites evolved in the heat-treated glass fiber was observed by a polarized optical microscope. In observation of cross-section of heat-treated glass fiber, the fiber fixed by a resin with ~250 μm in thickness was used as a sample.

The orientation axis of crystal in the first clad region was assumed by comparing the X-ray diffraction (XRD) (Cu Kα radiation) pattern of plate sample which is made from first clad glass with previous study.[7] For preparation of the measurement samples, the plate sample was heat-treated under $T_x - 30$ for 3 h, and the XRD measurement was tried on the as-prepared sample and surface polished sample. In addition, the powder sample treated at T_x for 3 h is also used on the measurement for determination of crystal phase.

The crystalline phase at the cross section was identified by micro Raman spectroscopy using an Ar^+ laser at 514.5 nm. Several points at the cross section of the treated fiber were examined, using $Ba_2TiGe_2O_8$, $Ba_2TiSi_2O_8$, and $BaTiGe_3O_9$, which were fabricated using a solid phase synthesis, as a reference.

3. Result and discussion

3.1 Crystallization behavior in double clad fibers

In this study, the heat-treatment temperature for crystallization process was firstly determined by a DTA measurement. As a result, T_x of the core, the first clad, and the second clad glasses were estimated to be 830°C, 789°C, and 807°C, respectively. Since the T_x of first clad glass showed the lowest value in these glasses, the selective crystallization in the first clad region is expected. **Figure 2** shows the cross section of the double clad fibers treated at the temperatures in the range from $T_x - 50$ K (739°C) to T_x (789°C). In the sample treated at $T_x - 50$ K, formation of the particle was observed at the boundary between the first- and the second-clad region. The particles have spherical shape with about 1 μm in diameter. The number of particles increased with the heat treatment temperature, and it was observed that the needle-like crystals were grown in the direction of both first-(inner) and second-clad (outer) glass from these particles. However, since the clear interference color could not be observed in the crystallized region, this result means that the orientation degree of crystallites is not so high.

3.2 Determination of crystal structure

Figure 3 shows XRD pattern of plate and powder samples made from the $30BaO{\cdot}15TiO_2{\cdot}30GeO_2{\cdot}25SiO_2{\cdot}1.0CuO$ crystallized glass with JCPDS data. The powder pattern (a) showed a fresnoite phase. The JCPDS data of $Ba_2TiGe_{1.2}Si_{0.8}O_8$, which has a diffraction pattern very similar to the obtained pattern (a), was selected to determine the plane indices. This result suggested that the obtained crystal includes a fresnoite crystal as mixed crystal that reflects the glass composition.

In the surface crystallized glass, it is reported that the degree of orientation is low just on the top of the surface.[10),11)] Also in this case, the as-prepared plate sample (b) did not clearly show the orientation of crystallites. After surface polishing, however, the c orientation was confirmed in the inner of the crystallized glass as shown in (c). The direct measurement of first clad region

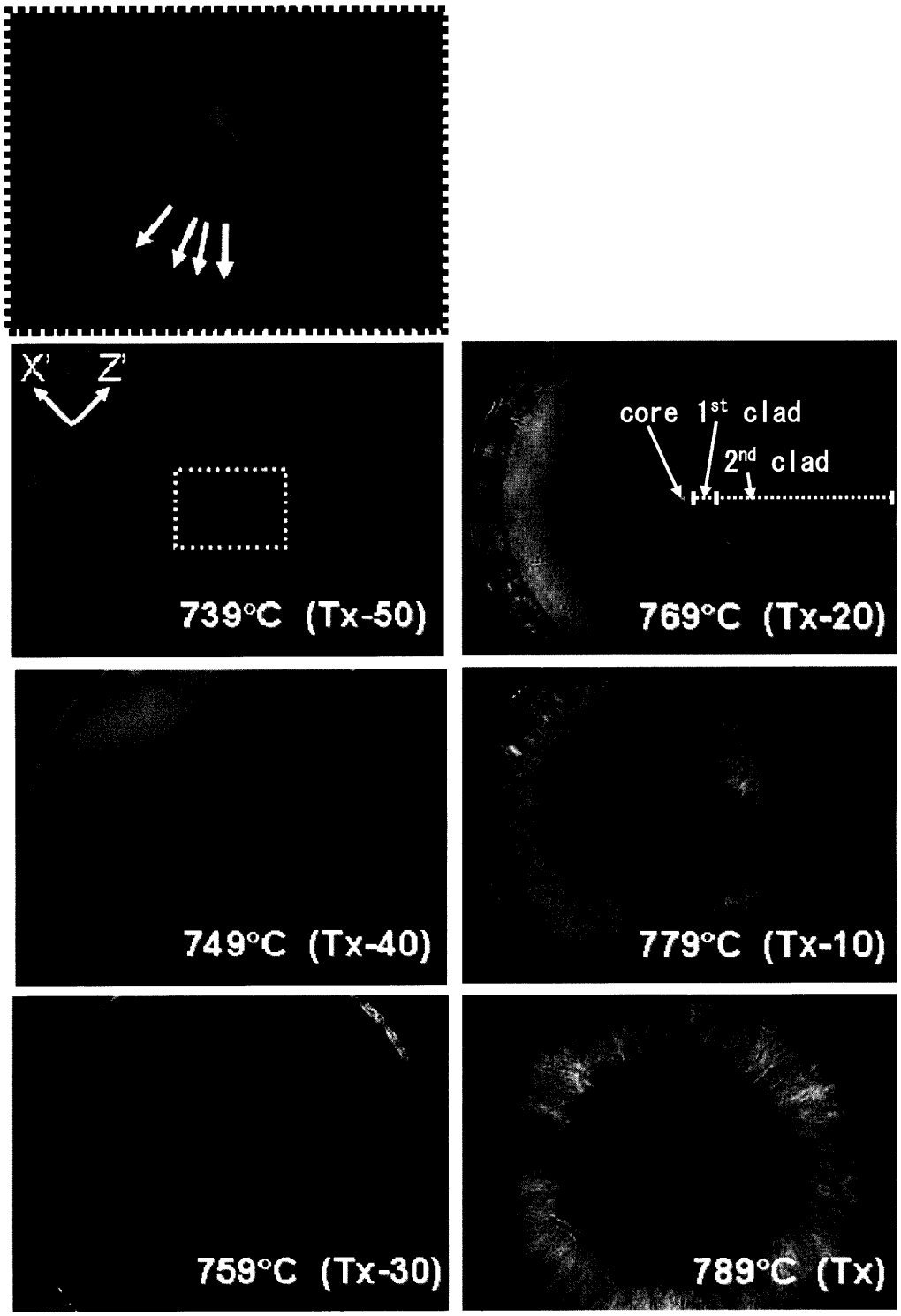

Fig. 2. Polarized optical micrograph for fibers obtained by a heat treatment at each treatment conditions. Arrows in a picture with dotted line frame shows starting points for crystal growth in first-second clad boundary.

in fiber samples was difficult because the first clad was covered by crystallized second clad. However, since the same orientation direction (c orientation) was found on the fiber and plane samples using the BTG55 glass,[7] this result means that the crystal obtained in this study would show the c orientation similar to bulk sample.

As a next step of the XRD measurement, we examined the crystalline phase at the cross section of the treated fibers with microscopic Raman spectroscopy. **Figure 4**(A) shows Raman spectra of the fiber sample treated at 769°C ($T_x - 20$ K). Several alphabetical marks in the figure indicate the different measurement spots on the cross section. Measurement point (a) is located at the core region whereas (b), (c), and (d) are different positions in the first clad region. On the other hand, (e) is the Raman spectrum of the $30BaO{\cdot}15TiO_2{\cdot}30GeO_2{\cdot}25SiO_2{\cdot}1.0CuO$ crystallized glass treated on T_x for 3 h. In the XRD measurement, we found

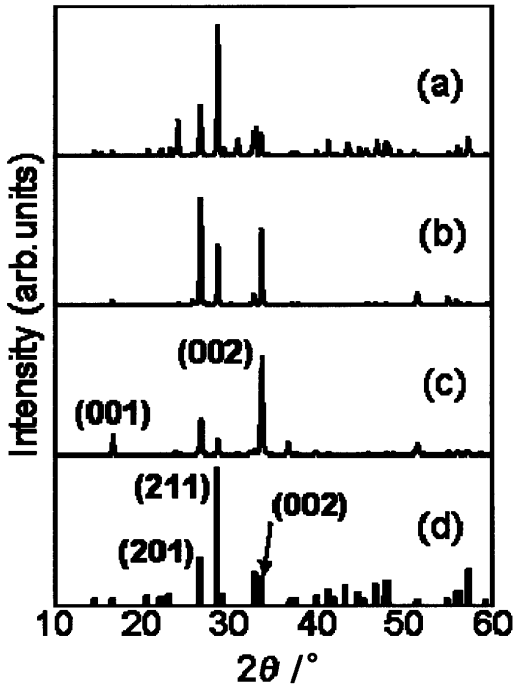

Fig. 3. XRD patterns for the $30BaO{\cdot}15TiO_2{\cdot}30GeO_2{\cdot}25SiO_2{\cdot}1.0CuO$ crystallized glass samples: (a) the powdered sample treated at 789°C (T_x) for 3 h, (b) the plate sample treated 759°C ($T_x - 30$ K) for 3 h, and (c) the surface-polished sample of (b). The data of JCPDS card (00-038-1245; $Ba_2TiGe_{1.2}Si_{0.8}O_8$) is also included.

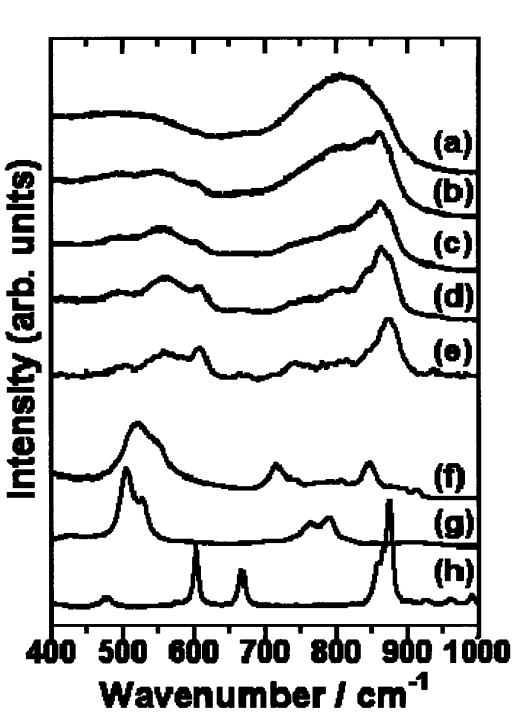

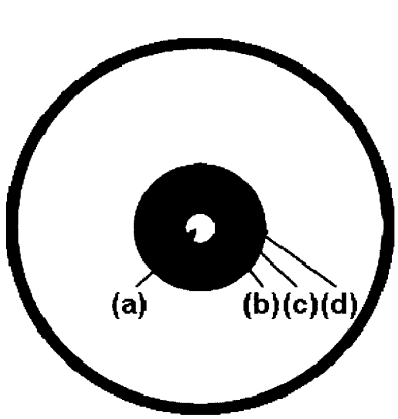

Fig. 4. Microscopic Raman scattering spectra for fiber obtained by heat treatment at $T_x - 20$ K (769°C) for 1 h (A), and schematic image of cross section of the fiber sample and the measurement points (B). (a) is the core section, and (b), (c), and (d) are first clad section at different positions. (e) is the reference sample treated on T_x for 3 h (f), (g), and (h) are also reference samples for ascription of Raman shift, $Ba_2TiGe_2O_8$, $BaTiGe_3O_9$, and $Ba_2TiSi_2O_8$ respectively.

that the precipitated crystalline phase in the first clad is fresnoite. However, in the $30BaO{\cdot}15TiO_2{\cdot}55GeO_2$ glass composition used in the previous study,[4] it was reported that benitoite phase crystal has been precipitated at the top of treated glass surface before growth of fresnoite phase crystal.[1] Therefore the Raman spectra of $Ba_2TiGe_2O_8$ (f), $BaTiGe_3O_9$ (g), and $Ba_2TiSi_2O_8$ (h), which were fabricated using a solid phase synthesis, were also measured for comparison.

Figure 4(B) shows schematic image of cross section of the fiber sample and the measurement points shown in the Fig. 6(A). In the core region (a), Raman spectrum showed broad peaks, which means that the core region was amorphous state without any crystallites. On the other hand, several peaks at 500–600 cm^{-1}, 650–700 cm^{-1}, 700–750 cm^{-1}, and 850–900 cm^{-1} are observed in (b), (c), and (d). These peaks are assigned to Ge–O–Ge symmetrical stretching vibration, Si–O–Si symmetrical stretching vibration, Ti–O stretching vibration, and Ti–O* stretching vibration, respectively.[12),13)]

Since no large difference was observed in intensity ratio between each peaks of measurement spots at (b), (c), and (d), it is considered that the composition change in crystallites is small. The benitoite phase was expected to be observed at the boundary surface whereas it was not shown clearly on this result. In addition, since the broad spectra that correspond with amorphous state appeared according to the movement of the measurement to the center of the cross section, it was indicated that the crystallization degree was small near the center. The geometric selection effect described later is the reason of the decrease of crystallization degree, that is, the decrease of growth-able crystallites number as crystallization progress. The low crystallization degree will be improved by a longer heat treatment.

3.3 Development of crystal orientation

The self-orientation of crystallites is often explained by the geometric selection effect with a probability theory.[5),6)] Although the direction of the crystal growth is random in the early stage,[10),11)] the preferential orientation of crystals in the direction perpendicular to the boundary occurs as the crystals progressively grow from the crystal nuclei. Here, the growth direction with fastest growth rate becomes to the orientation direction. In the theory, the population density of crystallites that has high orientation survived by the geometric selection effect n and the distance between neighbor crystallite h shows following relation,

$$n(h) \propto \frac{1}{\sqrt{h}}$$

This relation means that the high population density of crystal

nuclei, which provides the decrease of h, induces the increase of n, i.e. high orientation of crystallized layer. For the achievement of high population density of crystal nuclei, we have examined two-step heat-treatment that consists of the first heat-treatment for nucleation and the second treatment for crystal growth.

The optimal nucleation temperature of the first clad glass was determined using the DTA analysis with the same composition as the first clad.[14),15)] According to a report by Zhou and Yamane,[15)] the nucleation rate, I, is expressed by the equation $I = 1.052(E/R)(1/T_p - 1/T_{po}) + const$, where E is the activation energy for crystal growth, R is the gas constant, and T_{po} and T_p are the crystallization peak temperature of original glass and heat treated samples, respectively. The parameter $(1/T_p - 1/T_{po})$ is related to the nucleation rate and thus we can determine the temperature of maximum nucleation rate from a heat-treatment temperature vs $(1/T_p - 1/T_{po})$ curve. In this study, using the glass transition temperature (T_g: 688°C) as a basis for heat-treatment temperature, the glass of the first clad was heat-treated at several temperatures from $T_g - 20$ K to $T_g + 90$ K, each for 1 h. Using the heat-treated sample, DTA measurement was performed to measure the crystallization peak shift from untreated glass sample. In the DTA measurement, powdered samples were used to obtain large surface area, because inhomogeneous nucleation occurs at the surface of the glass. In **Fig. 5**, the values of $(1/T_p - 1/T_{po})$ are plotted against the heat-treatment temperature. If the maximal nucleation temperature of a glass is far from the crystallization peak, the curve of $1/T_p - 1/T_{po}$ has a peak at the temperature. In the present glass composition, however, no peak was observed before crystallization. We assume that the temperature of maximal nucleation is close to that of the crystallization peak. So, a higher temperature with low volume fraction of crystallites was used as the optimal temperature to decrease the crystal growth rate on the first nucleation step, because the crystal growth reduce the population density of crystal nuclei. The volume fraction of crystallites was estimated from the difference of crystallization peak area between heat-treated and un-treated samples. Estimated volume fraction of crystallites is also shown in Fig. 5 (square marks). Rapid increase of the crystal volume fraction is observed around 748°C ($T_g + 60$ K). Considering the guiding curve of the volume fraction, we selected 728°C ($T_g + 40$ K) as the optimal nucleation temperature in the glass of the first clad whereas 749°C ($T_x - 40$ K) as the crystallization peak temperature.

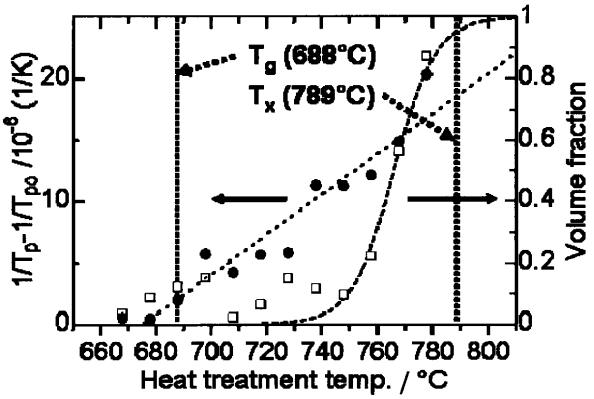

Fig. 5. Values of $(1/T_p - 1/T_{po})$ against heat-treatment temperature and volume fraction curve plotted by black circle and flamed square, respectively. Those lines are guide to eye.

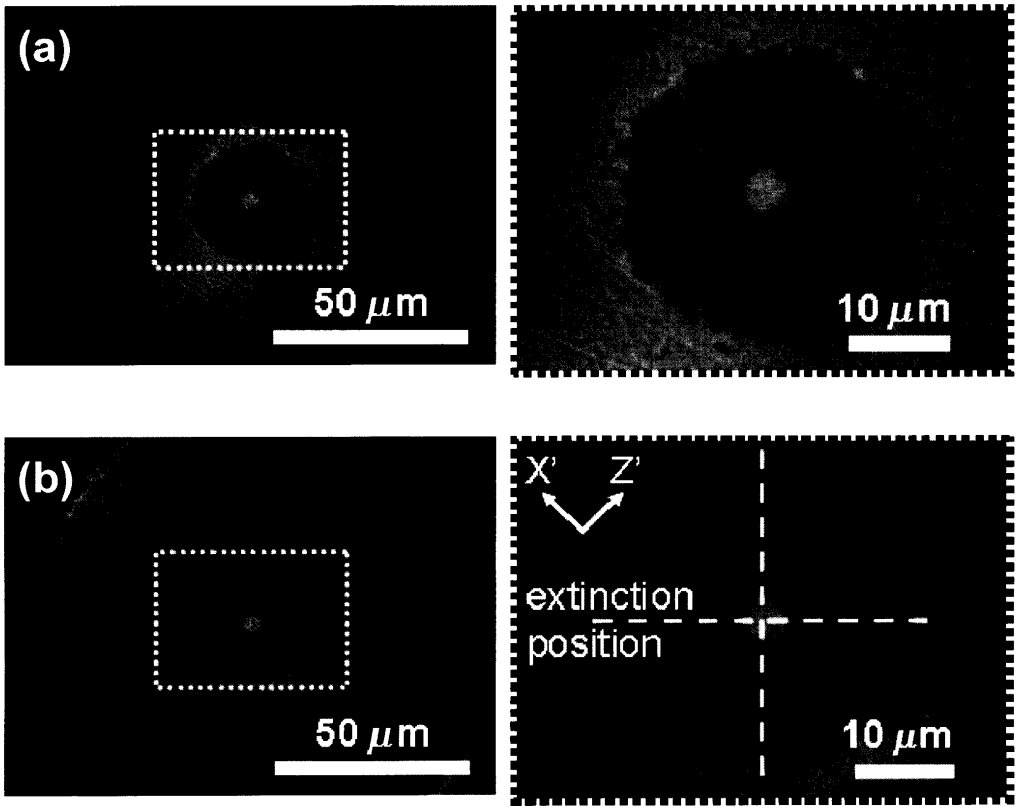

Fig. 6. Polarized optical micrograph for fibers obtained by nucleation at 728°C for 20 h (a) and crystallization at 749°C for 1 h after nucleation at 728°C for 20 h (b). The pictures with dotted line frame are extended figures to each core section.

Figure 6 shows polarization micrographs of cross sections of two crystallized fibers. One was heated to 698°C with 10 K/min, following by up to 728°C with 1 K/min, and kept at 728°C (T_g + 40 K) for 20 h (a). On the other hand, another was heated at 728°C for 20 hrs with the same heating program as (a), heated to 749°C with 1 K/min, and kept at 749°C (T_x – 40 K) for 1 h. In the picture (a), we found that many crystal particles were precipitated at the boundary between the first and the second clad. Note that the symmetric interference color is observed in the Fig. 6(a), which indicates high orientation of the crystallized phase from the boundary of clad to the center of the fiber. The symmetric interference color is also observed in the crystallized fiber (b) that was post heat-treated at 749°C for 1 h. Compared with the crystallized fiber with one step heat-treatment at 749°C (see Fig. 2), we found that the two step heat-treatment is effective for increasing of both nucleus population density and orientation of the crystallized phase of fresnoite.

4. Conclusion

We examined the crystallization behavior of double clad fibers fabricated from glass compositions to obtain the fresnoite type nonlinear optical crystallite. The measurement using XRD and Raman scattering showed that the oriented fresnoite type crystals are precipitated in first clad region from boundary between second clad to the center. In addition, it was found that the two step heat treatment for the increase of population density of crystal nuclei is effective to improve the crystal orientation.

References

1) Y. Takahashi, Y. Benino, T. Fujiwara and T. Komatsu, *Appl. Phys. Lett.*, 81[2], 223 (2002).
2) K. Narita, Y. Takahashi, Y. Benino, T. Fujiwara and T. Komatsu, *J. Am. Ceram. Soc.*, 87[1], 113–118 (2004).
3) K. Shioya, T. Komatsu, H. G. Kim, R. Sato and K. Matusita, *J. Non-Cryst. Solids*, 189, 16–24 (1995).
4) Y. Takahashi, K. Saitoh, Y. Benino, T. Fujiwara and T. Komatsu, *J. Non-Cryst. Solids*, 345&346, 412–416 (2004).
5) G. G. Lemmlein, *Dokl. Acad. Nauk SSSR*, 48, 177 (1945).
6) A. N. Kolmogorov, *Dokl. Acad. Nauk SSSR*, 65, 681–684 (1949).
7) Y. Hane, T. Komatsu, Y. Benino and T. Fujiwara, *J. Appl. Phys.*, 103, 063512 (2008).
8) H. Masai, Y. Takahasi, T. Fujiwara, S. Ohara, Y. Kondo and N. Sugimoto, submitted to *J. Mater. Res.*
9) S. Ohara, H. Masai, Y. Takahashi, T. Fujiwara, Y. Kondo and N. Sugimoto, submitted to *J. Ceram. Soc. Japan.*
10) H. Masai, T. Fijiwara, Y. Benini and T. Komatsu, *J. Appl. Phys.*, 100, 023526 (2006).
11) Y. Takahashi, Y. Benino, V. Dimitrov and T. Komatsu, *J. Non-Cryst. Solids*, 260, 155–159 (1999).
12) S. A. Markgraf and S. K. Sharma, *J. Am. Ceram. Soc.*, 75[9], 2630 (1992).
13) S. A. Markgraf and S. K. Sharma, *J. Mater. Res.*, 8[3], 635 (1993).
14) A. Marotta, A. Buri and F. Branda, *J. Mater. Sci.*, 16, 341 (1981).
15) X. Zhou and M. Yamane, *J. Ceram. Soc. Japan*, 96, 152 (1988).